Numerical Approximation of the inviscid 3D primitive equations in a limited domain

Ming-Cheng Shiue (National Chiao Tung University)

Joint work with
Qingshan Chen (Clemson University)
Roger Temam (Indiana University)
Joseph Tribbia (National Center for Atmospheric Research)

Central Weather Bureau, Taipei, Taiwan
Feburary 23, 2017

Outline

1. Introduction
   - Background, motivation and Difficulties
2. Limited area models based on the shallow water equations
   - Boundary conditions
   - Numerical implementation
3. Limited area models based on the primitive equations
   - Boundary conditions
   - Numerical implementation
4. Summary

Outline

Outline

Outline

Introduction:

Limited Area Models(LAMs) are often used to achieve high resolution over a region of interest. Examples are:

- Regional weather forecast,
- Simulation of coastal flows and gulf streams.

Challenge: lateral boundary conditions(LBCs)
No physical laws can provide natural boundary conditions at the lateral boundary. Furthermore, for computational purposes, we want the lateral boundary conditions to be transparent.

Figure 1: Transparent property

Introduction:

Limited Area Models(LAMs) are often used to achieve high resolution over a region of interest. Examples are:

- Regional weather forecast,
- Simulation of coastal flows and gulf streams.

Challenge: lateral boundary conditions(LBCs)

No physical laws can provide natural boundary conditions at the lateral boundary. Furthermore, for computational purposes, we want the lateral boundary conditions to be transparent.

Figure 1: Transparent property

Difficulty for LBCs

Difficulty:

- On the computational side
  Errors at the lateral boundary will propagate and advect into the modeled domain and have a major impact inside the domain.
- On the mathematical side
  Oliger and Sundstrom, 1978 showed the ill-posedness of a class of equations of geophysical fluid mechanics supplemented with any set of local boundary conditions. This class of equations includes the inviscid Primitive equations and the Shallow Water equations in the multi-layer case.

Difficulty for LBCs

Difficulty:

- On the computational side
  Errors at the lateral boundary will propagate and advect into the modeled domain and have a major impact inside the domain.
- On the mathematical side
  Oliger and Sundstrom, 1978 showed the ill-posedness of a class of equations of geophysical fluid mechanics supplemented with any set of local boundary conditions. This class of equations includes the inviscid Primitive equations and the Shallow Water equations in the multi-layer case.

The equation:

$$\frac{\partial u}{\partial t} + a\frac{\partial u}{\partial x} = 0.$$

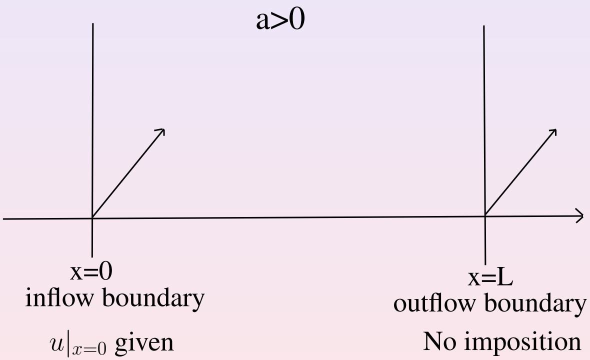

Figure 2: Boundary Conditions

Limited Area models based on the Shallow Water equations

Equations:

$$
\begin{cases}
\dfrac{\partial u}{\partial t} + u\dfrac{\partial u}{\partial x} + g\dfrac{\partial h}{\partial x} - fv = -g\dfrac{\partial B}{\partial x}, \quad x \in (0, L),\ t > 0, \\[2ex]
\dfrac{\partial v}{\partial t} + u\dfrac{\partial v}{\partial x} + fu = 0, \\[2ex]
\dfrac{\partial h}{\partial t} + u\dfrac{\partial h}{\partial x} + \dfrac{\partial u}{\partial x}h = 0.
\end{cases}
\tag{1}
$$

Initial conditions:

$$
u(x,0) = u_0(x), v(x,0) = v_0(x), h(x,0) = h_0(x), 0 < x < L. \tag{2}
$$

$$\begin{cases} \text{(u,v): } \textit{velocity}, \\ \text{h: the height of water level and} \\ \text{B: the height of the bottom.} \end{cases}$$

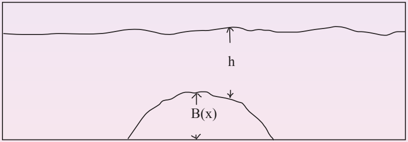

Figure 3: The shallow water model

Characteristic boundary conditions:

Consider the Shallow Water equations linearized around the simple uniform flow:

$$\bar{u} = u_0,\ \bar{v} = v_0,\ \text{and } \bar{h} = h_0.$$

We set

$$\begin{cases} u = \bar{u} + \tilde{u}, \\ v = \bar{v} + \tilde{v}, \\ h = \bar{h} + \tilde{h}. \end{cases}$$

$$\text{(LSWEs)} \begin{cases} \tilde{u}_t + u_0 \tilde{u}_x + g\tilde{h}_x - f\tilde{v} = 0, \\ \tilde{v}_t + u_0 \tilde{v}_x + f\tilde{u} = 0, \\ \tilde{h}_t + u_0 \tilde{h}_x + h_0 \tilde{u}_x = 0. \end{cases} \tag{3}$$

Perturbed Energy

Consider

$$\frac{d}{dt}\int_0^L (\tilde{u}^2 + \tilde{v}^2 + \frac{g}{h_0}\tilde{h}^2)\,dx = I(0,t) - I(L,t),$$

where

$$\begin{aligned}
I(x,t) &= u_0(\tilde{u}^2(x,t) + \tilde{v}^2(x,t) + \frac{g}{h_0}\tilde{h}^2(x,t)) + 2g\tilde{u}(x,t)\tilde{h}(x,t), \\
&= \begin{pmatrix} \tilde{u} & \tilde{v} & \frac{\sqrt{g}}{\sqrt{h_0}}\tilde{h} \end{pmatrix} \begin{pmatrix} u_0 & 0 & \sqrt{gh_0} \\ 0 & u_0 & 0 \\ \sqrt{gh_0} & 0 & u_0 \end{pmatrix} \begin{pmatrix} \tilde{u} \\ \tilde{v} \\ \frac{\sqrt{g}}{\sqrt{h_0}}\tilde{h} \end{pmatrix}, \\
&= (u_0 - \sqrt{gh_0})\tilde{\alpha}^2(x,t) + u_0\tilde{\beta}^2(x,t) + (u_0 + \sqrt{gh_0})\tilde{\gamma}^2(x,t),
\end{aligned}$$

where

$$
\begin{cases}
\tilde{\alpha}(x,t) = \dfrac{\tilde{u}(x,t)}{\sqrt{2}} - \sqrt{\dfrac{g}{2h_0}}\tilde{h}(x,t),\\
\tilde{\beta}(x,t) = \tilde{v}(x,t),\\
\tilde{\gamma}(x,t) = \dfrac{\tilde{u}(x,t)}{\sqrt{2}} + \sqrt{\dfrac{g}{2h_0}}\tilde{h}(x,t).
\end{cases}
$$

Flow type:

Subcritical flows: $u_0 - \sqrt{gh_0} < 0$

Supercritical flows : $u_0 - \sqrt{gh_0} > 0$

For subcritical flows:

$$
\begin{cases}
\tilde{u}(L,t) - \sqrt{\dfrac{g}{h_0}}\tilde{h}(L,t) = 0,\\
\tilde{v}(0,t) = 0,\\
\tilde{u}(0,t) + \sqrt{\dfrac{g}{h_0}}\tilde{h}(0,t) = 0.
\end{cases}
$$

For supercritical flows:

$$
\begin{cases}
\tilde{u}(0,t) - \sqrt{\dfrac{g}{h_0}}\tilde{h}(0,t) = 0,\\
\tilde{v}(0,t) = 0,\\
\tilde{u}(0,t) + \sqrt{\dfrac{g}{h_0}}\tilde{h}(0,t) = 0.
\end{cases}
$$

Linear type of characteristic boundary conditions:

For subcritical flows:

$$(I)\begin{cases}\alpha_1(L,t) = u(L,t) - \sqrt{\frac{g}{h_0}}h(L,t) = u_0 - \sqrt{gh_0},\\ \beta_1(0,t) = v(0,t) = v_0,\\ \gamma_1(0,t) = u(0,t) + \sqrt{\frac{g}{h_0}}h(0,t) = u_0 + \sqrt{gh_0}.\end{cases} \tag{4}$$

For supercritical flows:

$$(II)\begin{cases}\alpha_1(0,t) = u(0,t) - \sqrt{\frac{g}{h_0}}h(0,t) = u_0 - \sqrt{gh_0},\\ \beta_1(0,t) = v(0,t) = v_0,\\ \gamma_1(0,t) = u(0,t) + \sqrt{\frac{g}{h_0}}h(0,t) = u_0 + \sqrt{gh_0}.\end{cases} \tag{5}$$

Nonlinear type of characteristic boundary conditions:

Inspired by the theoretical work presented in the book of Benzoni and Serre, we consider the boundary conditions

For subcritical flows:

$$(\mathrm{III}) \begin{cases} \alpha_2(L,t) = \dfrac{u(L,t)}{2} - \sqrt{gh(L,t)} = \dfrac{u_0}{2} - \sqrt{gh_0}, \\ \beta_2(0,t) = v(0,t) = v_0, \\ \gamma_2(0,t) = \dfrac{u(0,t)}{2} + \sqrt{gh(0,t)} = \dfrac{u_0}{2} + \sqrt{gh_0}. \end{cases} \tag{6}$$

For supercritical flows:

$$(\mathrm{IV}) \begin{cases} \alpha_2(0,t) = \dfrac{u(0,t)}{2} - \sqrt{gh(0,t)} = \dfrac{u_0}{2} - \sqrt{gh_0}, \\ \beta_2(0,t) = v(0,t) = v_0, \\ \gamma_2(0,t) = \dfrac{u(0,t)}{2} + \sqrt{gh(0,t)} = \dfrac{u_0}{2} + \sqrt{gh_0}. \end{cases} \tag{7}$$

Equations for α_2, β_2, γ_2

$$\begin{cases} \dfrac{\partial \alpha_2}{\partial t} + (\dfrac{3\alpha_2 + \gamma_2}{2})\dfrac{\partial \alpha_2}{\partial x} = \dfrac{f\beta_2 - gB_x}{2}, \\[2ex] \dfrac{\partial \beta_2}{\partial t} + (\alpha_2 + \gamma_2)\dfrac{\partial \beta_2}{\partial x} = -f(\alpha_2 + \gamma_2), \\[2ex] \dfrac{\partial \gamma_2}{\partial t} + (\dfrac{\alpha_2 + 3\gamma_2}{2})\dfrac{\partial \gamma_2}{\partial x} = \dfrac{f\beta_2 - gB_x}{2}. \end{cases} \tag{8}$$

Subcritical flow $(u_0 - \sqrt{gh_0} < 0)$

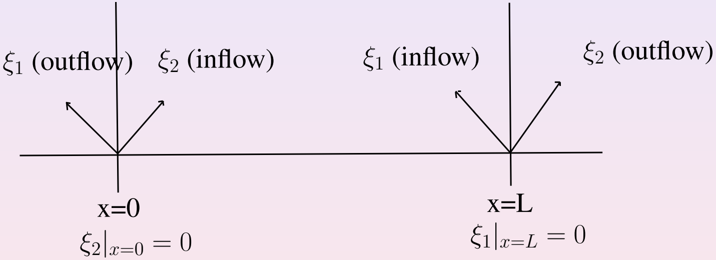

Figure 4:

Supercritical flow $(u_0 - \sqrt{gh_0} > 0)$

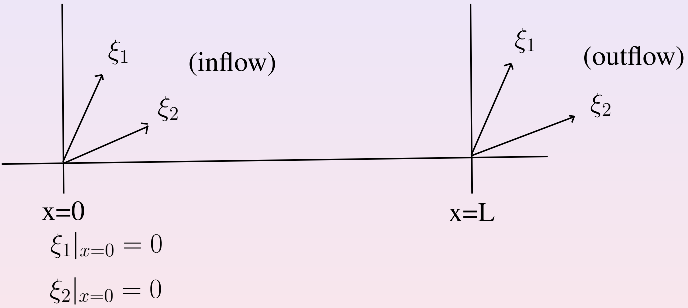

Figure 5:

Numerical schemes: semidiscrete central-upwind method

We rewrite the SWEs in conservative form as follows:

$$\frac{\partial}{\partial t}U + \frac{\partial}{\partial x}F(U) = S(U, t, x), \tag{9}$$

where

$$U = \begin{pmatrix} uh \\ vh \\ h \end{pmatrix}, \; F(U) = \begin{pmatrix} hu^2 + \frac{1}{2}gh^2 \\ uvh \\ uh \end{pmatrix}, \; S = \begin{pmatrix} fvh - gh\frac{\partial}{\partial x}B \\ -fuh \\ 0 \end{pmatrix}. \tag{10}$$

Numerical schemes: semidiscrete central-upwind method

Finite volume method:

$$\bar{U}_j(t) := \frac{1}{\Delta x} \int_{x_{j-\frac{1}{2}}}^{x_{j+\frac{1}{2}}} U(t,x)\,dx. \tag{11}$$

Discretized system:

$$\frac{d}{dt}\bar{U}_j(t) + \frac{F(U(t,x_{j+\frac{1}{2}})) - F(U(t,x_{j-\frac{1}{2}}))}{\Delta x} = \frac{\int_{x_{j-\frac{1}{2}}}^{x_{j+\frac{1}{2}}} S(U(t,x),t,x)dx}{\Delta x}. \tag{12}$$

Issues:

The approximation of the fluxes $F(U)$

The approximation of the source terms $S(U)$

The approximation of the fluxes

The approximations of the fluxes $F(U)$ at the points $x = x_{j\pm\frac{1}{2}}$ are given by

$$F(U(t, x_{j+\frac{1}{2}})) \approx F_{j+\frac{1}{2}}(t), \tag{13}$$

where

$$F_{j+\frac{1}{2}}(t) := \frac{a^{+}_{j+\frac{1}{2}} F(U^{-}_{j+\frac{1}{2}}) - a^{-}_{j+\frac{1}{2}} F(U^{+}_{j+\frac{1}{2}})}{a^{+}_{j+\frac{1}{2}} - a^{-}_{j+\frac{1}{2}}} + \frac{a^{+}_{j+\frac{1}{2}} a^{-}_{j+\frac{1}{2}}}{a^{+}_{j+\frac{1}{2}} - a^{-}_{j+\frac{1}{2}}} [U^{+}_{j+\frac{1}{2}} - U^{-}_{j+\frac{1}{2}}]. \tag{14}$$

Here $U^{+}_{j+\frac{1}{2}} := p_{j+1}(t, x_{j+\frac{1}{2}})$ and $U^{-}_{j+\frac{1}{2}} := p_j(t, x_{j+\frac{1}{2}})$, where $p_j(t, x)$ are non-oscillatory linear polynomial reconstructions

$$p_j(t, x) = \bar{U}_j + s_m(t)(x - x_j),$$

where

$$s_m(t) := minmod(\theta\frac{\bar{U}_{j+1}-\bar{U}_j}{\Delta x}, \frac{\bar{U}_{j+1}-\bar{U}_{j-1}}{2\Delta x}, \theta\frac{\bar{U}_j-\bar{U}_{j-1}}{\Delta x}), \quad (15)$$

with

$$minmod(x_1, x_2, \cdots) := \begin{cases} min(x_i), \text{ if } x_i > 0 \ \forall\, i, \\ max(x_i), \text{ if } x_i < 0 \ \forall\, i, \\ 0, \text{ otherwise }, \end{cases} \quad (16)$$

and $\theta \in [1, 2]$. Finally, the one-sided local speeds of propagation $a^{\pm}_{j+\frac{1}{2}}$ are given by

$$\begin{aligned} a^{+}_{j+\frac{1}{2}} &:= \max(\lambda_{\max}(\frac{\partial F}{\partial U}(U^{+}_{j+\frac{1}{2}})), \lambda_{\max}(\frac{\partial F}{\partial U}(U^{-}_{j+\frac{1}{2}})), 0), \\ a^{-}_{j+\frac{1}{2}} &:= \min(\lambda_{\min}(\frac{\partial F}{\partial U}(U^{+}_{j+\frac{1}{2}})), \lambda_{\min}(\frac{\partial F}{\partial U}(U^{-}_{j+\frac{1}{2}})), 0), \end{aligned} \quad (17)$$

where $\lambda_{\max}(\frac{\partial F}{\partial U}(\tilde{U}))$ and $\lambda_{\min}(\frac{\partial F}{\partial U}(\tilde{U}))$ are the largest and smallest eigenvalues of the differential $\frac{\partial F}{\partial U}$ at the point $U = \tilde{U}$.

The approximation of the source terms

Using the midpoint rule for the spatial integral:

$$\frac{1}{\Delta x}\int_{x_{j-\frac{1}{2}}}^{x_{j+\frac{1}{2}}} S(U(t,x),t,x)dx \approx S(U(t,x_j),t,x_j). \qquad (18)$$

ODE system:

$$\frac{d}{dt}\bar{U}_j(t) + \frac{F_{j+\frac{1}{2}}(t) - F_{j-\frac{1}{2}}(t)}{\Delta x} = S_j(t), \tag{19}$$

where

$$S_j(t) := S(U(t, x_j), t, x_j).$$

RK2 method:

$$\begin{cases} \dfrac{U_j^* - U_j^n}{\Delta t} = -\dfrac{F^n_{j+\frac{1}{2}} - F^n_{j-\frac{1}{2}}}{\Delta x} + S_j^n, \\ \dfrac{U_j^{**} - U_j^*}{\Delta t} = -\dfrac{F^*_{j+\frac{1}{2}} - F^*_{j-\frac{1}{2}}}{\Delta x} + S_j^*, \\ U_j^{n+1} = \dfrac{U_j^n + U_j^{**}}{2}. \end{cases} \tag{20}$$

Nonlinear type of characteristic boundary conditions:
For subcritical flows, $x = 0$,

$$\frac{\alpha_{2,1}^{n+1} - \alpha_{2,1}^{n}}{\Delta t} + \left(\frac{3\alpha_{2,1}^{n} + \gamma_{2,1}^{n}}{2}\right)\frac{\alpha_{2,2}^{n+1} - \alpha_{2,1}^{n+1}}{\Delta x} = \frac{f\beta_{2,1}^{n} - gB_{x,1}^{n}}{2}. \quad (21)$$

For subcritical flows, $x = L$,

$$\frac{\beta_{2,M+1}^{n+1} - \beta_{2,M+1}^{n}}{\Delta t} + (\alpha_{2,M+1}^{n} + \gamma_{2,M+1}^{n})\frac{\beta_{2,M+1}^{n+1} - \beta_{2,M}^{n+1}}{\Delta x} = -f(\alpha_{2,M+1}^{n} + \gamma_{2,M+1}^{n}), \quad (22)$$

and

$$\frac{\gamma_{2,M+1}^{n+1} - \gamma_{2,M+1}^{n}}{\Delta t} + \left(\frac{\alpha_{2,M+1}^{n} + 3\gamma_{2,M+1}^{n}}{2}\right)\frac{\gamma_{2,M+1}^{n+1} - \gamma_{2,M}^{n+1}}{\Delta x} = \frac{f\beta_{2,M+1}^{n} - gB_{x,M+1}^{n}}{2}. \quad (23)$$

For supercritical flows, $x = L$,

$$\frac{\alpha_{2,M+1}^{n+1} - \alpha_{2,M+1}^{n}}{\Delta t} + (u_0 - \sqrt{gh_0})\frac{\alpha_{2,M+1}^{n+1} - \alpha_{2,M}^{n+1}}{\Delta x}$$
$$+(\frac{3\alpha_{2,M+1}^{n} + \gamma_{2,M+1}^{n}}{4} - u_0 + \frac{\sqrt{gh_0}}{2})\frac{\alpha_{2,M+1}^{n} - \alpha_{2,M}^{n}}{\Delta x}$$
$$+(\frac{\alpha_{2,M+1}^{n} - \gamma_{2,M+1}^{n}}{4} + \frac{\sqrt{gh_0}}{2})\frac{\gamma_{2,M+1}^{n} - \gamma_{2,M}^{n}}{\Delta x} = f\beta_{2,M+1}^{n} - gB_{x,M+1}^{n}, \tag{24}$$

along with (22) and (23).

Numerical examples:

Subcritical flows:

Initial Conditions:

$$u(x,0) = u_0,\ v(x,0) = v_0,\ h(x,0) = \begin{cases} h_0 - B(x) + \epsilon\, h_0, & \text{if } \kappa \le x \le 2\kappa, \\ h_0 - B(x), & \text{otherwise .} \end{cases}$$

Here $u_0 = 0$ m/s , $v_0 = 0$ m/s , $h_0 = 10^4$ m and $\epsilon = 0.2$. The bottom topography consists of one hump,

$$B(x) = \begin{cases} \frac{\delta}{2} + \frac{\delta}{2} \cos\left(\frac{\pi(x - \frac{L}{2})}{\kappa}\right), & \text{if } |x - \frac{L}{2}| \le \kappa, \\ 0, & \text{otherwise ,} \end{cases}$$

where $\delta = 5 \times 10^3$ m, $\kappa = L/10$, and $L = 10^6$ m.

Simulation:

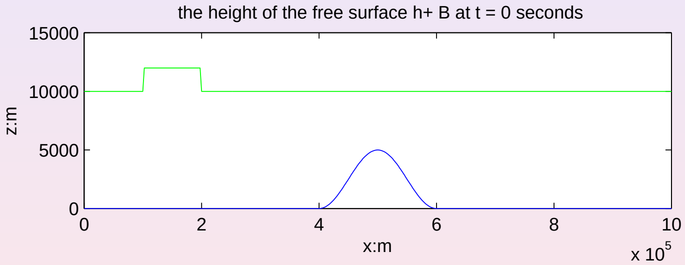
the height of the free surface h+ B at t = 0 seconds
15000
10000
5000
0
z:m
0
2
4
6
8
10
x:m
x 10^5

Initial Conditions:

$$u(x,0) = u_0,\ v(x,0) = v_0,\ h(x,0) = h_0 - B(x).$$

Here $u_0 = 450$ m/s , $v_0 = 0$ m/s , $h_0 = 5 \times 10^3$ m . The bottom topography consists of one hump,

$$B(x) = \begin{cases} \frac{\delta}{2} + \frac{\delta}{2}\cos\left(\frac{\pi(x - \frac{L}{2})}{\kappa}\right), & \text{if } |x - \frac{L}{2}| \leq \kappa, \\ 0, & \text{otherwise}, \end{cases}$$

where $\delta = 2.5 \times 10^3$ m, $\kappa = L/10$, and $L = 10^6$ m.

Supercritical Flows: nonlinear type boundary conditions

Simulation:

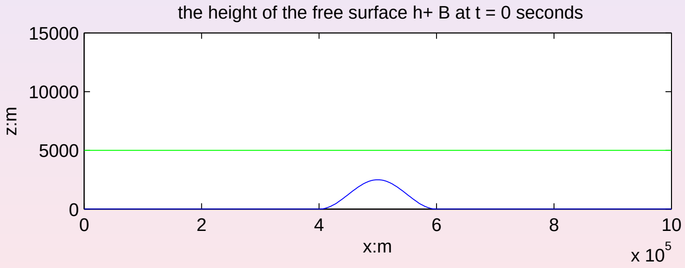

The Model Equations

The 3D inviscid Primitive Equations :

$$\begin{cases} \dfrac{\partial \tilde{\mathbf{v}}}{\partial t} + (\tilde{\mathbf{v}} \cdot \nabla)\tilde{\mathbf{v}} + \tilde{w}\dfrac{\partial \tilde{\mathbf{v}}}{\partial z} + f\mathrm{k} \times \tilde{\mathbf{v}} + \dfrac{1}{\rho_0}\nabla \tilde{p} = 0, \text{(Momentum equation)} \\ \dfrac{\partial \tilde{p}}{\partial z} = -\tilde{\rho} g, \ \text{(Hydrostatic equation)} \\ \nabla \cdot \tilde{\mathbf{v}} + \dfrac{\partial \tilde{w}}{\partial z} = 0, \ \text{(Continuity equation)} \\ \dfrac{\partial \tilde{T}}{\partial t} + (\tilde{\mathbf{v}} \cdot \nabla)\tilde{T} + \tilde{w}\dfrac{\partial \tilde{T}}{\partial z} = 0, \ \text{(Thermodynamics equation)} \\ \tilde{\rho} = \rho_0(1 - \alpha(\tilde{T} - T_0)). \text{(Equation of states)} \end{cases} \tag{25}$$

$\tilde{\mathbf{v}}$:	$= (\tilde{u}, \tilde{v})$ the horizontal velocity	$\tilde{w}$:	the vertical velocity
$\tilde{\rho}$:	the density	$\tilde{p}$:	the pressure
∇ :	the horizontal gradient operator	$\tilde{T}$:	the temperature

Previous Work

- Rousseau, Temam, and Tribbia, 2005 and 2007 - an infinite set of nonlocal boundary conditions for the 2D inviscid PEs, well-posedness for the linearized equations, and computation for the nonlinear equations.
- Chen, Laminie, Rousseau, Temam and Tribbia 2008, Chen, Temam and Tribbia 2009: analysis and computation of the 2.5D case.
- Rousseau, Temam and Tribbia 2008: well-posedness of the linearized 3D inviscid PEs.

Previous Work

- Rousseau, Temam, and Tribbia, 2005 and 2007 - an infinite set of nonlocal boundary conditions for the 2D inviscid PEs, well-posedness for the linearized equations, and computation for the nonlinear equations.
- Chen, Laminie, Rousseau, Temam and Tribbia 2008, Chen, Temam and Tribbia 2009: analysis and computation of the 2.5D case.
- Rousseau, Temam and Tribbia 2008: well-posedness of the linearized 3D inviscid PEs.

Previous Work

- Rousseau, Temam, and Tribbia, 2005 and 2007 - an infinite set of nonlocal boundary conditions for the 2D inviscid PEs, well-posedness for the linearized equations, and computation for the nonlinear equations.
- Chen, Laminie, Rousseau, Temam and Tribbia 2008, Chen, Temam and Tribbia 2009: analysis and computation of the 2.5D case.
- Rousseau, Temam and Tribbia 2008: well-posedness of the linearized 3D inviscid PEs.

The domain under consideration is $\mathcal{M} = \mathcal{M}' \times (0, -L_3)$, where $\mathcal{M}' = (0, L_1) \times (0, L_2)$.

Linearization around the simple uniform stratified flow :

$$\begin{aligned} \bar{u} &= \bar{U}_0,\ \bar{v} = 0,\ \bar{w} = 0, \\ \bar{T} &= \frac{N^2}{\alpha g} z,\ \bar{\rho} = -\frac{\rho_0 N^2}{g} z,\ \frac{d\bar{P}(z)}{dz} = -(\rho_0 + \bar{\rho}) g, \end{aligned}$$

where $\bar{U}_0$, ρ_0, and T_0 are positive constants and we introduce the Brunt–Väisälä (buoyancy) frequency

$$N^2 = \frac{g}{\rho_0} \frac{d\bar{\rho}}{dz}.$$

In this work, we assume that N is a positive constant. Setting:

$$\begin{aligned} \tilde{u} &= \bar{u} + u(x, y, z, t), & \tilde{T} &= T_0 + \bar{T}(z) + T(x, y, z, t) \\ \tilde{v} &= \bar{v} + v = v(x, y, z, t), & \tilde{\rho} &= \rho_0 + \bar{\rho}(z) + \rho(x, y, z, t), \\ \tilde{w} &= \bar{w} + w = w(x, y, z, t), & \tilde{p} &= p_0 + \bar{p}(z) + p(x, y, z, t) \end{aligned}$$

Linearization around the simple uniform stratified flow

The domain under consideration is $\mathcal{M} = \mathcal{M}' \times (0, -L_3)$, where $\mathcal{M}' = (0, L_1) \times (0, L_2)$.
Linearization around the simple uniform stratified flow :

$$\begin{aligned} \bar{u} &= \bar{U}_0,\ \bar{v} = 0,\ \bar{w} = 0, \\ \bar{T} &= \frac{N^2}{\alpha g} z,\ \bar{\rho} = -\frac{\rho_0 N^2}{g} z,\ \frac{d\bar{P}(z)}{dz} = -(\rho_0 + \bar{\rho}) g, \end{aligned}$$

where $\bar{U}_0$, ρ_0, and T_0 are positive constants and we introduce the Brunt–Väisälä (buoyancy) frequency

$$N^2 = \frac{g}{\rho_0} \frac{d\bar{\rho}}{dz}.$$

In this work, we assume that N is a positive constant. Setting:

$$\begin{aligned} \tilde{u} &= \bar{u} + u(x,y,z,t), & \tilde{T} &= T_0 + \bar{T}(z) + T(x,y,z,t) \\ \tilde{v} &= \bar{v} + v = v(x,y,z,t), & \tilde{\rho} &= \rho_0 + \bar{\rho}(z) + \rho(x,y,z,t), \\ \tilde{w} &= \bar{w} + w = w(x,y,z,t), & \tilde{p} &= p_0 + \bar{p}(z) + p(x,y,z,t) \end{aligned}$$

The domain under consideration is $\mathcal{M} = \mathcal{M}' \times (0, -L_3)$, where $\mathcal{M}' = (0, L_1) \times (0, L_2)$.
Linearization around the simple uniform stratified flow :

$$\begin{aligned} \bar{u} &= \bar{U}_0,\ \bar{v} = 0,\ \bar{w} = 0, \\ \bar{T} &= \frac{N^2}{\alpha g} z,\ \bar{\rho} = -\frac{\rho_0 N^2}{g} z,\ \frac{d\bar{P}(z)}{dz} = -(\rho_0 + \bar{\rho})g, \end{aligned}$$

where $\bar{U}_0$, ρ_0, and T_0 are positive constants and we introduce the Brunt–Väisälä (buoyancy) frequency

$$N^2 = \frac{g}{\rho_0}\frac{d\bar{\rho}}{dz}.$$

In this work, we assume that N is a positive constant. Setting:

$$\begin{aligned} \tilde{u} &= \bar{u} + u(x,y,z,t), & \tilde{T} &= T_0 + \bar{T}(z) + T(x,y,z,t) \\ \tilde{v} &= \bar{v} + v = v(x,y,z,t), & \tilde{\rho} &= \rho_0 + \bar{\rho}(z) + \rho(x,y,z,t), \\ \tilde{w} &= \bar{w} + w = w(x,y,z,t), & \tilde{p} &= p_0 + \bar{p}(z) + p(x,y,z,t). \end{aligned}$$

System

We have the following equations for u, v, w, $\phi = p/\rho_0$, and $\psi = \phi_z = \alpha g T$:

$$
\begin{cases}
u_t + \bar{U}_0 u_x - fv + \phi_x + B(u, v, w; u) = 0, \\
v_t + \bar{U}_0 v_x + fu + \phi_y + fu + B(u, v, w; v) + f\bar{U}_0 = 0, \\
\phi_z = -\dfrac{\rho}{\rho_0} g = \psi, \\
u_x + v_y + w_z = 0, \\
\psi_t + \bar{U}_0 \psi_x + N^2 w + B(u, v, w; \psi) = 0,
\end{cases}
\tag{26}
$$

where

$$
B(u, v, w; \theta) = u\theta_x + v\theta_y + w\theta_z, \ \text{for } \theta = u,\ v,\ \text{or } \psi.
$$

The Linearized system

$$\begin{cases} u_t + \bar{U}_0 u_x - fv + \phi_x = 0, \\ v_t + \bar{U}_0 v_x + fu + \phi_y = 0, \\ \phi_z = \psi, \\ u_x + v_y + w_z = 0, \\ \psi_t + \bar{U}_0 \psi_x + N^2 w = 0. \end{cases} \quad (27)$$

Separation of variables:

$$\begin{cases} u(x,y,z,t) = \mathcal{U}(z)\hat{u}(x,y,t), \; v(x,y,z,t) = \mathcal{V}(z)\hat{v}(x,y,t), \\ \psi(x,y,z,t) = \Psi(z)\hat{\psi}(x,y,t), \\ w(x,y,z,t) = \mathcal{W}(z)\hat{w}(x,y,t), \; \phi(x,y,z,t) = \Phi(z)\hat{u}(x,y,t), \end{cases}$$

For simplicity, we take

$$\mathcal{U} = \mathcal{V} = \Phi, \; \mathcal{W} = \Psi.$$

$$\begin{cases} u_t + \bar{U}_0 u_x - fv + \phi_x = 0, \\ v_t + \bar{U}_0 v_x + fu + \phi_y = 0, \\ \phi_z = \psi, \\ u_x + v_y + w_z = 0, \\ \psi_t + \bar{U}_0 \psi_x + N^2 w = 0. \end{cases} \tag{27}$$

Separation of variables:

$$\begin{cases} u(x,y,z,t) = \mathcal{U}(z)\hat{u}(x,y,t),\ v(x,y,z,t) = \mathcal{V}(z)\hat{v}(x,y,t), \\ \psi(x,y,z,t) = \Psi(z)\hat{\psi}(x,y,t), \\ w(x,y,z,t) = \mathcal{W}(z)\hat{w}(x,y,t),\ \phi(x,y,z,t) = \Phi(z)\hat{u}(x,y,t), \end{cases}$$

For simplicity, we take

$$\mathcal{U} = \mathcal{V} = \Phi,\ \mathcal{W} = \Psi.$$

The Linearized system

$$\begin{cases} u_t + \bar{U}_0 u_x - fv + \phi_x = 0, \\ v_t + \bar{U}_0 v_x + fu + \phi_y = 0, \\ \phi_z = \psi, \\ u_x + v_y + w_z = 0, \\ \psi_t + \bar{U}_0 \psi_x + N^2 w = 0. \end{cases} \tag{27}$$

Separation of variables:

$$\begin{cases} u(x,y,z,t) = \mathcal{U}(z)\hat{u}(x,y,t),\ v(x,y,z,t) = \mathcal{V}(z)\hat{v}(x,y,t), \\ \psi(x,y,z,t) = \Psi(z)\hat{\psi}(x,y,t), \\ w(x,y,z,t) = \mathcal{W}(z)\hat{w}(x,y,t),\ \phi(x,y,z,t) = \Phi(z)\hat{u}(x,y,t), \end{cases}$$

For simplicity, we take

$$\mathcal{U} = \mathcal{V} = \Phi,\ \mathcal{W} = \Psi.$$

The Linearized system

From the third and fourth equations in (27), we find that the corresponding Sturm-Liouville problems are as follows:

$$\mathcal{U}'' + \lambda^2 \mathcal{U} = 0,\ \mathcal{W}'' + \lambda^2 \mathcal{W} = 0,$$

with the following natural boundary conditions:

$$\mathcal{U}'(0) = \mathcal{U}'(-L_3) = 0,\ \mathcal{W}(0) = \mathcal{W}(-L_3) = 0.$$

The boundary conditions come from the following top and bottom boundary conditions:

$$w(z = 0) = w(z = -L_3) = 0.$$

The Linearized system

From the third and fourth equations in (27), we find that the corresponding Sturm-Liouville problems are as follows:

$$\mathcal{U}'' + \lambda^2 \mathcal{U} = 0, \ \mathcal{W}'' + \lambda^2 \mathcal{W} = 0,$$

with the following natural boundary conditions:

$$\mathcal{U}'(0) = \mathcal{U}'(-L_3) = 0, \ \mathcal{W}(0) = \mathcal{W}(-L_3) = 0.$$

The boundary conditions come from the following top and bottom boundary conditions:

$$w(z = 0) = w(z = -L_3) = 0.$$

Normal Mode Expansion in z

We look for the general solutions of (26) in the form:

$$\begin{cases} (u, v, \phi) = \sum_{n \geq 0} \mathcal{U}_n(z)(u_n, v_n, \phi_n)(x, y, t), \\ (w, \psi) = \sum_{n \geq 1} \mathcal{W}_n(z)(w_n, \psi_n)(x, y, t). \end{cases} \tag{28}$$

where $\mathcal{U}_n(z)$ and $\mathcal{W}_n(z)$ are the eigenfunctions of the Sturm-Liouville problem associated with linearized equations of (26) and

$$\begin{cases} \lambda_n = \frac{n\pi}{L_3}, \\ \mathcal{W}_n(z) = \sqrt{\frac{2}{L_3}} \sin(\lambda_n z), \mathcal{U}_n(z) = \sqrt{\frac{2}{L_3}} \cos(\lambda_n z), n \geq 1, \\ \mathcal{U}_0(z) = \frac{1}{\sqrt{L_3}}. \end{cases} \tag{29}$$

The barotropic mode

For $n = 0$, we find that

$$\begin{cases} \dfrac{\partial u_0}{\partial t} + \bar{U}_0 \dfrac{\partial u_0}{\partial x} + \dfrac{\partial \phi_0}{\partial x} - f v_0 + \displaystyle\int_{-L_3}^{0} B(u, v, w; u)\,\mathcal{U}_0(z)\,dz = 0, \\ \dfrac{\partial v_0}{\partial t} + \bar{U}_0 \dfrac{\partial v_0}{\partial x} + \dfrac{\partial \phi_0}{\partial y} + f u_0 + \displaystyle\int_{-L_3}^{0} B(u, v, w; v)\,\mathcal{U}_0(z)\,dz \\ \hfill + f \bar{U}_0 \sqrt{L_3} = 0, \\ \hfill \dfrac{\partial u_0}{\partial x} + \dfrac{\partial v_0}{\partial y} = 0, \\ \hfill \psi_0 = w_0 = 0, \end{cases} \tag{30}$$

The higher modes

For $n \geq 1$, we find that

$$\begin{cases} \dfrac{\partial u_n}{\partial t} + \bar{U}_0 \dfrac{\partial u_n}{\partial x} - f v_n + \dfrac{\partial \phi_n}{\partial x} + \displaystyle\int_{-L_3}^{0} B(u, v, w; u)\, \mathcal{U}_n(z)\, dz = 0, \\ \dfrac{\partial v_n}{\partial t} + \bar{U}_0 \dfrac{\partial v_n}{\partial x} + f u_n + \dfrac{\partial \phi_n}{\partial y} + \displaystyle\int_{-L_3}^{0} B(u, v, w; v)\, \mathcal{U}_n(z)\, dz = 0, \\ \dfrac{\partial \psi_n}{\partial t} + \bar{U}_0 \dfrac{\partial \psi_n}{\partial x} + N^2 w_n + \displaystyle\int_{-L_3}^{0} B(u, v, w; \psi)\, \mathcal{W}_n(z)\, dz = 0, \\ \phi_n = -\dfrac{1}{\lambda_n} \psi_n, \; w_n = -\dfrac{1}{\lambda_n} \left(\dfrac{\partial u_n}{\partial x} + \dfrac{\partial v_n}{\partial y} \right). \end{cases} \tag{31}$$

$$\begin{cases} \dfrac{\partial u_n}{\partial t} + \bar{U}_0 \dfrac{\partial u_n}{\partial x} - f v_n - \dfrac{1}{\lambda_n} \dfrac{\partial \psi_n}{\partial x} = 0, \\ \dfrac{\partial v_n}{\partial t} + \bar{U}_0 \dfrac{\partial v_n}{\partial x} + f u_n - \dfrac{1}{\lambda_n} \dfrac{\partial \psi_n}{\partial y} = 0, \\ \dfrac{\partial \psi_n}{\partial t} + \bar{U}_0 \dfrac{\partial \psi_n}{\partial x} - \dfrac{N^2}{\lambda_n} (\dfrac{\partial u_n}{\partial x} + \dfrac{\partial v_n}{\partial y}) = 0. \end{cases} \tag{32}$$

We rewrite (32) in the matrix form as follows:

$$\frac{\partial U_n}{\partial t} + E_n \frac{\partial U_n}{\partial x} + F_n \frac{\partial U_n}{\partial y} = 0. \tag{33}$$

Here,

$$U_n = \begin{pmatrix} u_n \\ v_n \\ \psi_n \end{pmatrix}, E_n = \begin{pmatrix} \bar{U}_0 & 0 & \dfrac{-1}{\lambda_n} \\ 0 & \bar{U}_0 & 0 \\ \dfrac{-N^2}{\lambda_n} & 0 & \bar{U}_0 \end{pmatrix}, F_n = \begin{pmatrix} 0 & 0 & 0 \\ 0 & 0 & \dfrac{-1}{\lambda_n} \\ 0 & \dfrac{-N^2}{\lambda_n} & 0 \end{pmatrix}$$

(34)

The eigenvalues of the matrix E_n are

$$\bar{U}_0 - \frac{N}{\lambda_n},\ \bar{U}_0, \bar{U}_0 + \frac{N}{\lambda_n}.$$

We define n_c as the positive integer satisfying the following relations:

$$\frac{n_c \pi}{L_3} < \frac{N}{\bar{U}_0} < \frac{(n_c + 1)\pi}{L_3}.$$

The mode is subcritical if $1 \leq n \leq n_c$,

The mode is supercritical if $n > n_c$.

The eigenvalues of the matrix E_n are

$$\bar{U}_0 - \frac{N}{\lambda_n},\ \bar{U}_0, \bar{U}_0 + \frac{N}{\lambda_n}.$$

We define n_c as the positive integer satisfying the following relations:

$$\frac{n_c \pi}{L_3} < \frac{N}{\bar{U}_0} < \frac{(n_c + 1)\pi}{L_3}.$$

$$\text{The mode is subcritical if } 1 \leq n \leq n_c,$$
$$\text{The mode is supercritical if } n > n_c.$$

The matrix form for the zero mode is

$$\begin{cases} \mathbf{v}_t + \bar{U}_0 \mathbf{v}_x + f\mathrm{k} \times \mathbf{v} + \nabla \phi_0 + G_0 = 0, \\ \mathrm{div}\mathbf{v} = 0. \end{cases} \tag{35}$$

Here,
$\mathbf{v} = (u_0,\ v_0)^T$ and

$$G_0 = \begin{pmatrix} \int_{-L_3}^{0} B(u, v, w; u)\,\mathcal{U}_0(z)\,dz \\ \int_{-L_3}^{0} B(u, v, w; v)\,\mathcal{U}_0(z)\,dz + f\bar{U}_0\sqrt{L_3} \end{pmatrix}, \tag{36}$$

Boundary conditions for the zero mode

We propose the following boundary conditions:

$$\begin{cases} u_0 = 0, & \text{at } x = 0,\ L_1. \\ v_0 = 0, & \text{at } x = 0,\ \text{ and } y = 0,\ L_2. \end{cases} \tag{37}$$

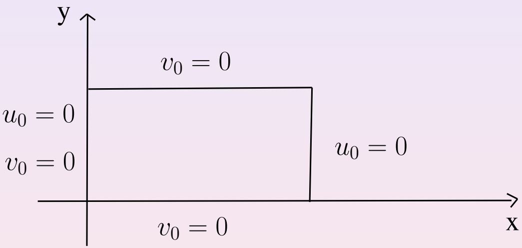

Figure 6: Boundary conditions for the zero mode

Remark 1

- *The initial boundary problem is not classical.*

Let $\Delta t = T/K$, $\mathbf{v}^k \approx \mathbf{v}(x, y, k\Delta t)$, and $\mathbf{v}^{k+\frac{1}{2}}$ represents an intermediate value between $\mathbf{v}^k$ and $\mathbf{v}^{k+1}$, etc.

First Step:

$$\begin{cases} \dfrac{\mathbf{v}^{k+\frac{1}{2}} - \mathbf{v}^k}{\Delta t} + \bar{U}_0 \mathbf{v}_x^{k+\frac{1}{2}} + f\mathbf{k} \times \mathbf{v}^k + \nabla \phi_0^k + G_0^k = 0, \\ \mathbf{v}^{k+\frac{1}{2}}|_{x=0} = 0, \end{cases} \tag{38}$$

Here

$$G_0^k = \begin{pmatrix} \int_{-L_3}^0 B(u^k, v^k, w^k; u^k)\mathcal{U}_0(z)\,dz \\ \int_{-L_3}^0 B(u^k, v^k, w^k; v^k)\mathcal{U}_0(z)\,dz + f\bar{U}_0\sqrt{L_3} \end{pmatrix}, \tag{39}$$

Second Step: (projection method)

$$\begin{cases} \dfrac{\mathbf{v}^{k+1} - \mathbf{v}^{k+\frac{1}{2}}}{\Delta t} + \nabla(\phi_0^{k+1} - \phi_0^k) = 0, \\ \nabla \cdot \mathbf{v}^{k+1} = 0, \\ \mathbf{v}^{k+1} \cdot \mathbf{n} = 0 \text{ on } \partial\mathcal{M}'. \end{cases} \tag{40}$$

Neumann Problem

From the Second Step, we can find ϕ_0^{k+1} by solving the Neumann problem

$$\begin{cases} \triangle\phi_0^{k+1} = \triangle\phi_0^{k} + \dfrac{\nabla\cdot\mathbf{v}^{k+\frac{1}{2}}}{\Delta t}, \\ \nabla\phi_0^{k+1}\cdot\mathbf{n} = \dfrac{\mathbf{v}^{k+\frac{1}{2}}}{\Delta t}, \quad \partial\mathcal{M}'. \end{cases} \tag{41}$$

and imposing the compatibility condition

$$\int_{\mathcal{M}'} \phi_0^{k+1}\,dx\,dy = 0.$$

Stability Issue

Given the mesh size $\mathbf{h} = (\Delta x, \Delta y)$, we have the following stability result:

Lemma 1

(Chen-Shiue-Temam-10) If Δt and $S(\mathbf{h})$ satisfy the conditions

$$\Delta t\, S^4(\mathbf{h}) \le \frac{1}{c_1^2 K_4}, \quad \Delta t \le \frac{1}{8}, \text{ where } S^2(\mathbf{h}) = \frac{1}{(\Delta x)^2} + \frac{1}{(\Delta y)^2}, \tag{42}$$

then, for $0 \le n \le N_T$, we have

$$|\mathbf{v}_{\mathbf{h}}^n|_{\mathbf{h}}^2 \le K_4, \quad (\Delta t)^3 \sum_{k=1}^{N_T} |\nabla_{\mathbf{h}} \phi_{\mathbf{h}}^k|_{\mathbf{h}}^2 \le K_4. \tag{43}$$

We rewrite (31) in the matrix form as follows:

$$\frac{\partial U_n}{\partial t} + E_n \frac{\partial U_n}{\partial x} + F_n \frac{\partial U_n}{\partial y} + G_n = 0. \tag{44}$$

Here,

$$U_n = \begin{pmatrix} u_n \\ v_n \\ \psi_n \end{pmatrix}, E_n = \begin{pmatrix} \bar{U}_0 & 0 & \frac{-1}{\lambda_n} \\ 0 & \bar{U}_0 & 0 \\ \frac{-N^2}{\lambda_n} & 0 & \bar{U}_0 \end{pmatrix}, F_n = \begin{pmatrix} 0 & 0 & 0 \\ 0 & 0 & \frac{-1}{\lambda_n} \\ 0 & \frac{-N^2}{\lambda_n} & 0 \end{pmatrix} \tag{45}$$

and

$$G_n = \begin{pmatrix} -fv_n + \int_{-H}^{0} B(u,v,w;u)\mathcal{U}_n(z)dz \\ fu_n + \int_{-H}^{0} B(u,v,w;v)\mathcal{U}_n(z)dz \\ \int_{-H}^{0} B(u,v,w;\psi)\mathcal{W}_n(z)dz \end{pmatrix}. \tag{46}$$

Change Variables

Change variables:

$$\begin{pmatrix} \xi_n \\ v_n \\ \eta_n \end{pmatrix} = \begin{pmatrix} u_n - \dfrac{\psi_n}{N} \\ v_n \\ u_n + \dfrac{\psi_n}{N} \end{pmatrix}, \begin{pmatrix} u_n \\ \alpha_n \\ \beta_n \end{pmatrix} = \begin{pmatrix} u_n \\ v_n + \dfrac{\psi_n}{N} \\ v_n - \dfrac{\psi_n}{N} \end{pmatrix}. \tag{47}$$

Boundary conditions for the subcritical modes:

$$\begin{cases} \xi_n(0, y, t) = 0, \\ v_n(0, y, t) = 0, \\ \eta_n(L_1, y, t) = 0. \end{cases} \quad \begin{cases} \alpha_n(x, L_2, t) = 0, \\ \beta_n(x, 0, t) = 0. \end{cases} \tag{48}$$

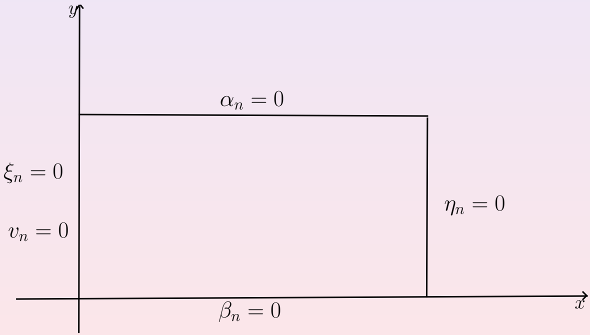

Figure 7: Boundary conditions for the subcritical modes

Boundary conditions for the supercritical modes:

$$\begin{cases} \xi_n(0, y, t) = 0, \\ v_n(0, y, t) = 0, \\ \eta_n(0, y, t) = 0. \end{cases} \quad \begin{cases} \alpha_n(x, L_2, t) = 0, \\ \beta_n(x, 0, t) = 0. \end{cases} \tag{49}$$

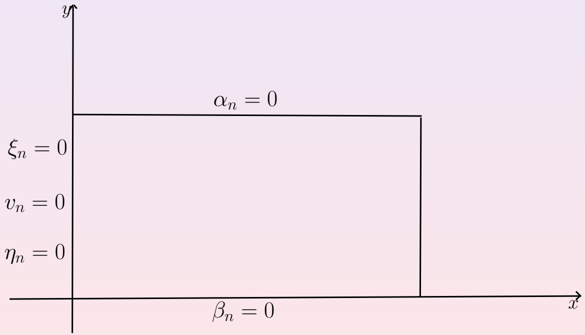

Figure 8: Boundary conditions for the supercritical modes

Well-posedness issues for the subcritical and supercritical modes

Remark 2

- *The boundary conditions* (48) *and* (49) *are different from those proposed in RTT08.*
- *The well-posedness of the linearized equations will be studied elsewhere.*

Numerical Schemes for the subcritical modes

Splitting method:

The First Step:

$$\frac{U_n^{k+\frac{1}{2}} - U_n^k}{\Delta t} + E_n \frac{\partial U_n^{k+\frac{1}{2}}}{\partial x} + G_n^k = 0. \tag{50}$$

The Second Step:

$$\frac{U_n^{k+1} - U_n^{k+\frac{1}{2}}}{\Delta t} + F_n \frac{\partial U_n^{k+1}}{\partial y} = 0. \tag{51}$$

Remark 3

- *This is a partly implicit scheme.*

Numerical scheme for the subcritical modes

The First Step:

$$\begin{cases} \dfrac{\xi_{n,i,j}^{k+\frac{1}{2}} - \xi_{n,i,j}^{k}}{\Delta t} + (\bar{U}_0 + \dfrac{N}{\lambda_n}) \dfrac{\xi_{n,i,j}^{k+\frac{1}{2}} - \xi_{n,i-1,j}^{k+\frac{1}{2}}}{\Delta x} = S_{n,i,j}^{k,1}, i = 2, \cdots, I+1, \\ \dfrac{v_{n,i,j}^{k+\frac{1}{2}} - v_{n,i,j}^{k}}{\Delta t} + \bar{U}_0 \dfrac{v_{n,i,j}^{k+\frac{1}{2}} - v_{n,i-1,j}^{k+\frac{1}{2}}}{\Delta x} = S_{n,i,j}^{k,2}, i = 2, \cdots, I+1, \\ \dfrac{\eta_{n,i,j}^{k+\frac{1}{2}} - \eta_{n,i,j}^{k}}{\Delta t} + (\bar{U}_0 - \dfrac{N}{\lambda_n}) \dfrac{\eta_{n,i+1,j}^{k+\frac{1}{2}} - \eta_{n,i,j}^{k+\frac{1}{2}}}{\Delta x} = S_{n,i,j}^{k,3}, i = 1, \cdots, I, \\ \qquad \text{and } j = 1, \cdots, J+1 \text{ in all cases,} \end{cases} \tag{52}$$

where

$$S_{n,i,j}^{K,1},\ S_{n,i,j}^{k,2} \text{ and } S_{n,i,j}^{k,2} \text{ are nonlinear terms.}$$

Numerical scheme for the subcritical modes

The boundary conditions for $\xi_n^{k+\frac{1}{2}}$, $v_n^{k+\frac{1}{2}}$ and $\eta_n^{k+\frac{1}{2}}$ are

$$\xi_{n,0,j}^{k+\frac{1}{2}} = 0, \quad v_{n,0,j}^{k+\frac{1}{2}} = 0, \quad \eta_{n,I,j}^{k+\frac{1}{2}} = 0, \quad \text{for } 0 \le j \le J, \tag{53}$$

The Second Step

$$\begin{cases} \dfrac{u_{n,i,j}^{k+1} - u_{n,i,j}^{k+\frac{1}{2}}}{\Delta t} = 0, \\ \dfrac{\alpha_{n,i,j}^{k+1} - \alpha_{n,i,j}^{k+\frac{1}{2}}}{\Delta t} - \dfrac{N}{\lambda_n} \dfrac{\alpha_{n,i,j+1}^{k+1} - \alpha_{n,i,j}^{k+1}}{\Delta y} = 0, \\ \dfrac{\beta_{n,i,j}^{k+1} - \beta_{n,i,j}^{k+\frac{1}{2}}}{\Delta t} + \dfrac{N}{\lambda_n} \dfrac{\beta_{n,i,j}^{k+1} - \beta_{n,i,j-1}^{k+1}}{\Delta y} = 0 \end{cases} \tag{54}$$

The boundary conditions for α_n^{k+1}, β_n^{k+1} are

$$\begin{cases} \alpha_{n,I,j}^{k+1} = 0, & \text{for } 0 \le j \le J, \\ \beta_{n,i,0}^{k+1} = 0, & \text{for } 0 \le i \le I. \end{cases} \tag{55}$$

Numerical schemes for the supercritical modes

Splitting method:

The First Step:

$$\begin{cases} \dfrac{\xi_{n,i,j}^{k+\frac{1}{2}} - \xi_{n,i,j}^{k}}{\Delta t} + (\bar{U}_0 + \dfrac{N}{\lambda_n}) \dfrac{\xi_{n,i,j}^{k+\frac{1}{2}} - \xi_{n,i-1,j}^{k+\frac{1}{2}}}{\Delta x} = S_{n,i,j}^{k,1}, i = 2, \cdots, I+1, \\ \dfrac{v_{n,i,j}^{k+\frac{1}{2}} - v_{n,i,j}^{k}}{\Delta t} + \bar{U}_0 \dfrac{v_{n,i,j}^{k+\frac{1}{2}} - v_{n,i-1,j}^{k+\frac{1}{2}}}{\Delta x} = S_{n,i,j}^{k,2}, i = 2, \cdots, I+1, \\ \dfrac{\eta_{n,i,j}^{k+\frac{1}{2}} - \eta_{n,i,j}^{k}}{\Delta t} + (\bar{U}_0 - \dfrac{N}{\lambda_n}) \dfrac{\eta_{n,i,j}^{k+\frac{1}{2}} - \eta_{n,i-1,j}^{k+\frac{1}{2}}}{\Delta x} = S_{n,i,j}^{k,3}, i = 1, \cdots, I, \\ \qquad \text{and } i = 1, \cdots, J+1 \text{ in all cases}, \end{cases} \tag{56}$$

The boundary conditions for $\xi_n^{k+\frac{1}{2}}$, $v_n^{k+\frac{1}{2}}$ and $\eta_n^{k+\frac{1}{2}}$ are, for $0 \le j \le J$,

$$\xi_{n,0,j}^{k+\frac{1}{2}} = 0, \quad v_{n,0,j}^{k+\frac{1}{2}} = 0, \quad \eta_{n,0,j}^{k+\frac{1}{2}} = 0. \tag{57}$$

The second Step:

$$\begin{cases} \dfrac{u_{n,i,j}^{k+1} - u_{n,i,j}^{k+\frac{1}{2}}}{\Delta t} = 0, \\ \dfrac{\alpha_{n,i,j}^{k+1} - \alpha_{n,i,j}^{k+\frac{1}{2}}}{\Delta t} - \dfrac{N}{\lambda_n} \dfrac{\alpha_{n,i,j+1}^{k+1} - \alpha_{n,i,j}^{k+1}}{\Delta y} = 0, \\ \dfrac{\beta_{n,i,j}^{k+1} - \beta_{n,i,j}^{k+\frac{1}{2}}}{\Delta t} + \dfrac{N}{\lambda_n} \dfrac{\beta_{n,i,j}^{k+1} - \beta_{n,i,j-1}^{k+1}}{\Delta y} = 0 \end{cases} \tag{58}$$

The boundary conditions for α_n^{k+1}, β_n^{k+1} are

$$\begin{cases} \alpha_{n,I,j}^{k+1} = 0, & \text{for } 0 \leq j \leq J, \\ \beta_{n,i,0}^{k+1} = 0, & \text{for } 0 \leq i \leq I. \end{cases} \tag{59}$$

Treatment of the integral of the nonlinear term

In our study, we only need to consider a small number of modes (≤ 10), and it is then appropriate to transform these integrals into the sums of the Fourier coefficients.

Numerical Simulations in a nested domain

Consider two domains as follows:
The larger domain:

$$\mathcal{M} = (0, L_1) \times (0, L_2) \times (-L_3, 0)$$

The middle-half domain:

$$\mathcal{M}_1 = (L_1/4, 3L_1/4) \times (L_2/4, 3L_2/4) \times (-L_3, 0)$$

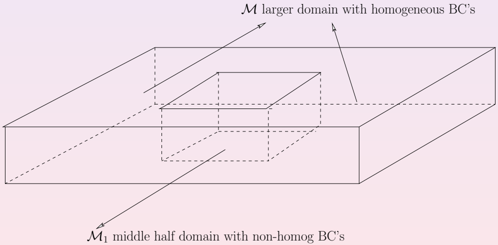

Figure 9: The larger domain $\mathcal{M}$ and the middle half domain $\mathcal{M}_1$.

Numerical simulations in a nested domain

Strategies:

1. Given the initial and boundary conditions, we perform simulations on the larger domain.
2. We perform simulations on the middle-half domain using the initial and boundary conditions provided from Step 1.
3. We consider the data from Step 1 as the true solution, compare these two data from Step 1 and Step 2 in the middle-half domain and compute relative errors.

Numerical Experiments

In the simulation, the initial conditions are given by these scalar functions:

$$
\begin{cases}
u(x,y,z,0) = \dfrac{x}{L_1}\dfrac{2\pi}{L_2}\sin\left(\dfrac{2\pi x}{L_1}\right)\cos\left(\dfrac{2\pi y}{L_2}\right) + \sin\left(\dfrac{4\pi x}{L_1}\right)\cos\left(\dfrac{4\pi y}{L_2}\right) \\
\qquad\qquad\qquad \cos\left(\dfrac{\pi z}{H}\right), \\
v(x,y,z,0) = \dfrac{-1}{L_1}\left(\sin\left(\dfrac{2\pi x}{L_1}\right) + \dfrac{2\pi x}{L_1}\cos\left(\dfrac{2\pi x}{L_1}\right)\right)\sin\left(\dfrac{2\pi y}{L_2}\right) \\
\qquad\qquad\qquad + \dfrac{L_2}{L_1}\left(\sin^2\left(\dfrac{4\pi x}{L_1}\right) + \sin\left(\dfrac{4\pi x}{L_1}\right)\sin\left(\dfrac{4\pi y}{L_2}\right)\cos\left(\dfrac{\pi z}{H}\right)\right), \\
w(x,y,z,0) = \dfrac{-4H}{L_1}\left(\sin\left(\dfrac{4\pi x}{L_1}\right) + \cos\left(\dfrac{4\pi x}{L_1}\right)\right)\cos\left(\dfrac{4\pi y}{L_2}\right)\sin\left(\dfrac{\pi z}{H}\right), \\
\phi(x,y,z,0) = \bar{U}_0\sin\left(\dfrac{2\pi x}{L_1}\right)\sin\left(\dfrac{2\pi y}{L_2}\right)\left(\cos\left(\dfrac{\pi z}{H}\right) - \cos\left(\dfrac{2\pi z}{H}\right)\right), \\
\psi(x,y,z,0) = \dfrac{\pi\bar{U}_0}{H}\sin\left(\dfrac{2\pi x}{L_1}\right)\sin\left(\dfrac{2\pi y}{L_2}\right)\left(2\sin\left(\dfrac{2\pi z}{H}\right) - \sin\left(\dfrac{\pi z}{H}\right)\right).
\end{cases}
\tag{60}
$$

Numerical Experiments

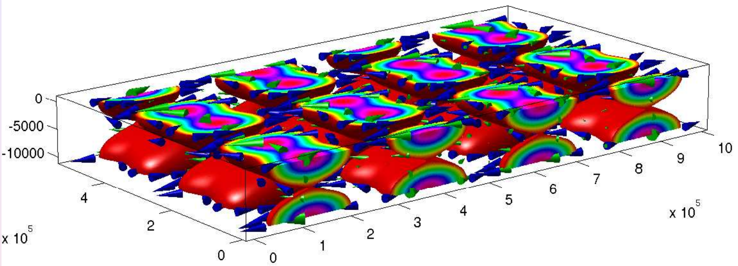

Figure 10: Initial conditions for velocity field

Numerical Experiments

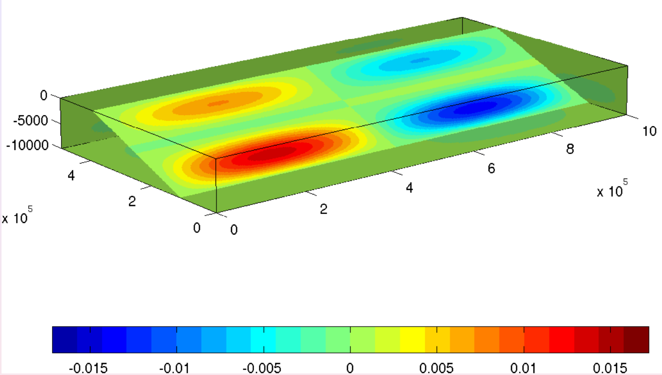

Figure 11: Initial conditions for ϕ

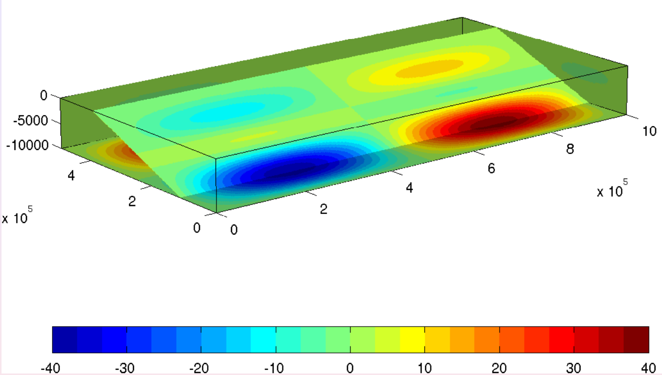

Figure 12: Initial conditions for ψ

Numerical simulations in the larger domain

Boundary conditions: homogeneous conditions
for the *zero mode*,

$$\begin{cases} u_0(0, y, t) = 0, \quad u_0(L_1, y, t) = 0, \\ v_0(0, y, t) = 0, \quad v_0(x, 0, t) = 0, \quad v_0(x, L_2, t) = 0; \end{cases} \tag{61}$$

for the *subcritical modes*, i.e. when $1 \leq n < n_c$,

$$\begin{cases} \xi_n(0, y, t) = 0, \quad v_n(0, y, t) = 0, \quad \eta_n(L_1, y, t) = 0, \\ \alpha_n(x, L_2, t) = 0, \quad \beta_n(x, 0, t) = 0; \end{cases} \tag{62}$$

and for the *supercritical modes*, i.e. when $n > n_c$,

$$\begin{cases} \xi_n(0, y, t) = 0, \quad v_n(0, y, t) = 0, \quad \eta_n(0, y, t) = 0, \\ \alpha_n(x, L_2, t) = 0, \quad \beta_n(x, 0, t) = 0. \end{cases} \tag{63}$$

The physical parameters:

$$
\begin{array}{cl}
\text{The length of the domain in } x-\text{direction} & L_1 = 10^3 \text{ km}, \\
\text{The length of the domain in } y-\text{direction} & L_2 = 500 \text{ km}, \\
\text{The length of the domain in } z-\text{direction} & L_3 = 10 \text{ km}, \\
\text{The constant reference velocity} & \bar{U}_0 = 20\text{m/s}, \\
\text{The Coriolis parameter} & f = 10^{-4}, \\
\text{The Brunt–Väisälä (buoyancy) frequency} & N = 10^{-2}, \\
\text{The final time} & T = 5 \times 10^4 \text{ s}, \\
\text{The number of modes} & N_{max} = 5.
\end{array}
$$

Numerical simulations in the larger domain

The numerical parameters:

$$\begin{array}{rl} \text{The number of time steps} & N_T = 1600, \\ \text{The number of mesh grids in } x & N_x = 400, \\ \text{The number of mesh grids in } y & N_y = 200, \\ \text{The number of mesh grids in } z & N_z = 40. \end{array}$$

Numerical Experiments in the larger domain

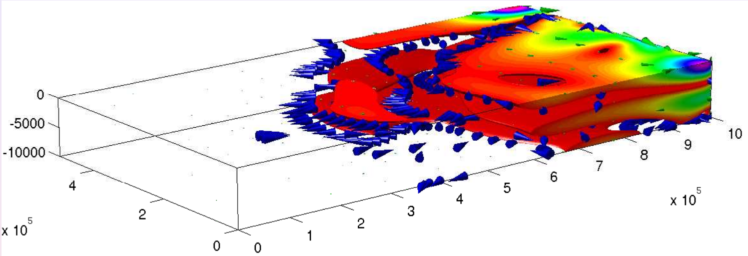

Figure 13: Numerical results for velocity field

Numerical Experiments in the larger domain

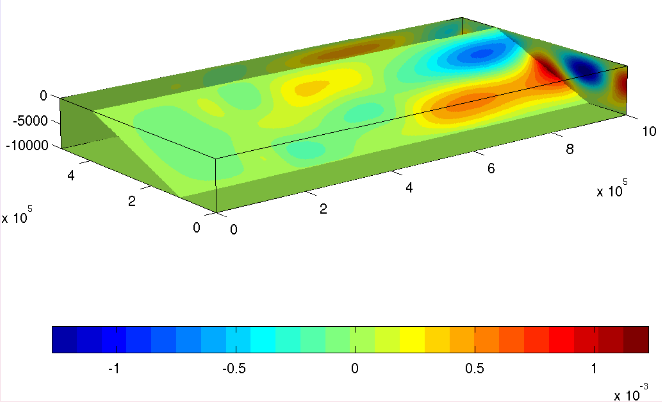

Figure 14: Numerical results for ϕ

Numerical Experiments in the larger domain

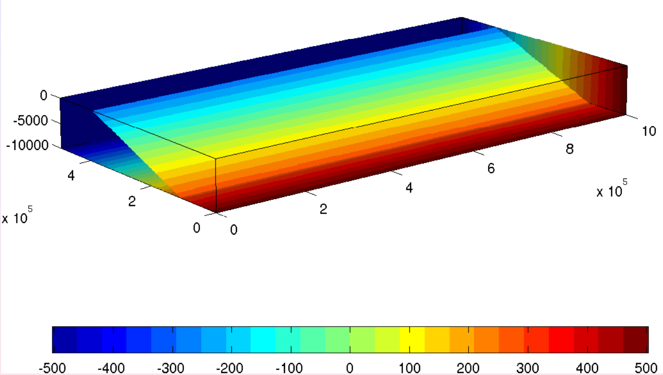

Figure 15: Numerical results for ψ

Boundary conditions:
for the *zero mode*,

$$\begin{cases} u_0(L_1/4, y_j, t_k) = u_0^I(L_1/4, y_j, t_k), \\ u_0(3L_1/4, y_j, t_k) = u_0^I(3L_1/4, y_j, t_k), \\ v_0(L_1/4, y_j, t_k) = v_0^I(L_1/4, y_j, t_k), \\ v_0(x_i, L_2/4, t_k) = v_0^I(x_i, L_2/4, t_k), \\ v_0(x_i, 3L_2/4, t_k) = v_0^I(x_i, 3L_2/4, t_k). \end{cases} \tag{64}$$

for the *subcritical modes*, i.e. when $1 \leq n < n_c$,

$$\begin{cases} \xi_n(L_1/4, y_j, t_k) = \xi_n^I(L_1/4, y_j, t_k), \\ v_n(L_1/4, y_j, t_k) = v_n^I(L_1/4, y_j, t_k), \\ \eta_n(3L_1/4, y_j, t_k) = \eta_n^I(3L_1/4, y_j, t_k), \\ \alpha_n(x_i, 3L_2/4, t_k) = \alpha_n^I(x_i, 3L_2/4, t_k), \\ \beta_n(x_i, L_2/4, t_k) = \beta_n^I(x_i, L_2/4, t_k), \end{cases} \tag{65}$$

and for the *supercritical modes*, i.e. when $n > n_c$,

$$\begin{cases} \xi_n(L_1/4, y_j, t_k) = \xi_n^l(L_1/4, y_j, t_k), \\ v_n(L_1/4, y_j, t_k) = v_n^l(L_1/4, y_j, t_k), \\ \eta_n(L_1/4, y_j, t_k) = \eta_n^l(L_1/4, y_j, t_k), \\ \alpha_n(x_i, 3L_2/4, t_k) = \alpha_n^l(x_i, 3L_2/4, t_k), \\ \beta_n(x_i, L_2/4, t_k) = \beta_n^l(x_i, L_2/4, t_k). \end{cases} \tag{66}$$

The numerical parameters:

$$
\begin{aligned}
\text{The number of time steps} \quad & N_T = 1600, \\
\text{The number of mesh grids in } x \quad & N_x = 200, \\
\text{The number of mesh grids in } y \quad & N_y = 100, \\
\text{The number of mesh grids in } z \quad & N_z = 40.
\end{aligned}
$$

Numerical Experiments in the middle-half domain

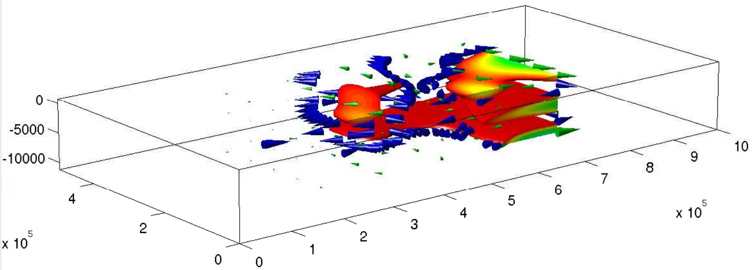

Figure 16: Numerical results for velocity field

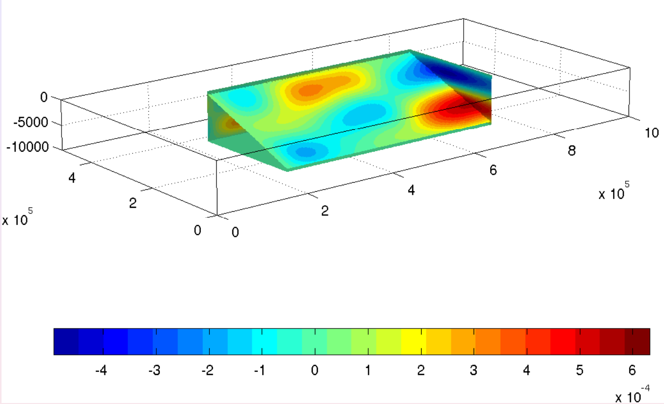

Figure 17: Numerical results for ϕ

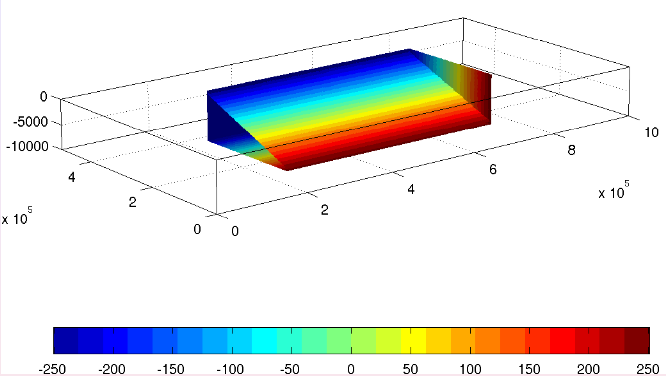

Figure 18: Numerical results for ψ

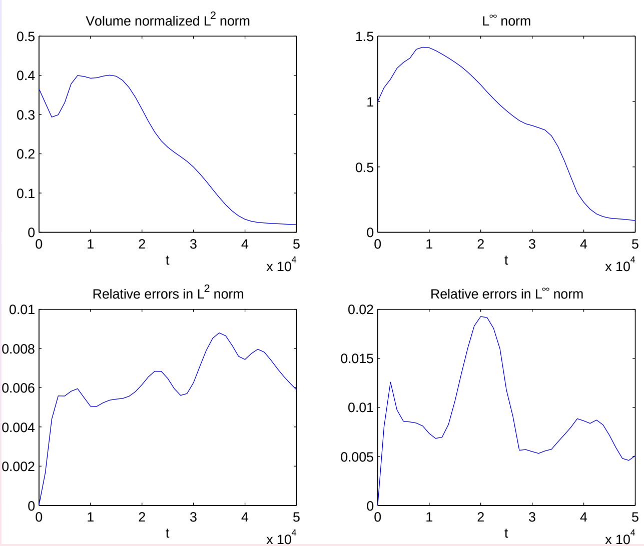

Figure 19: Top row: evolution of the solution u in the L^2 and L^∞ norms. Bottom row: evolution of the relative errors for u in the L^2 and L^∞ norms.

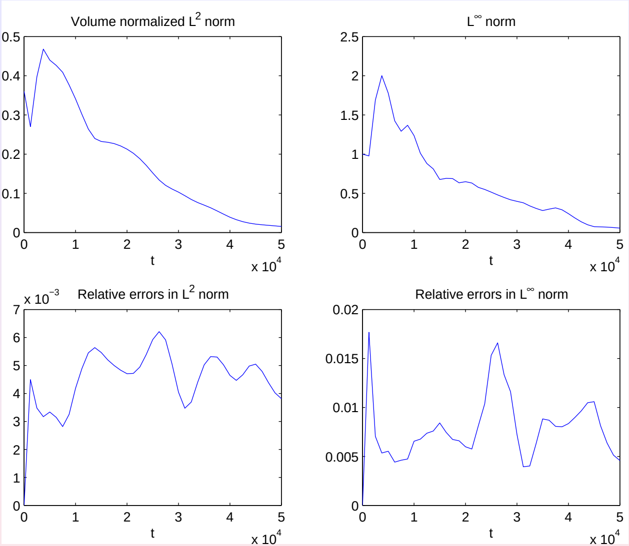

Figure 20: Top row: evolution of the solution v in the L^2 and L^∞ norms. Bottom row: evolution of the relative errors for v in the L^2 and L^∞ norms.

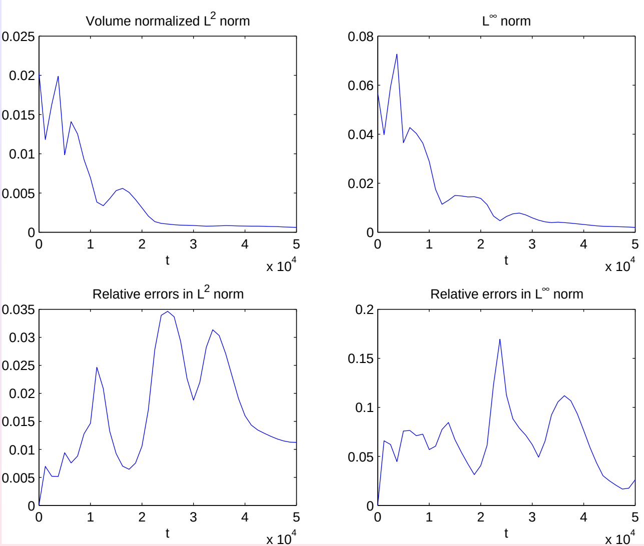

Figure 21: Top row: evolution of the solution w in the L^2 and L^∞ norms. Bottom row: evolution of the relative errors for w in the L^2 and L^∞ norms.

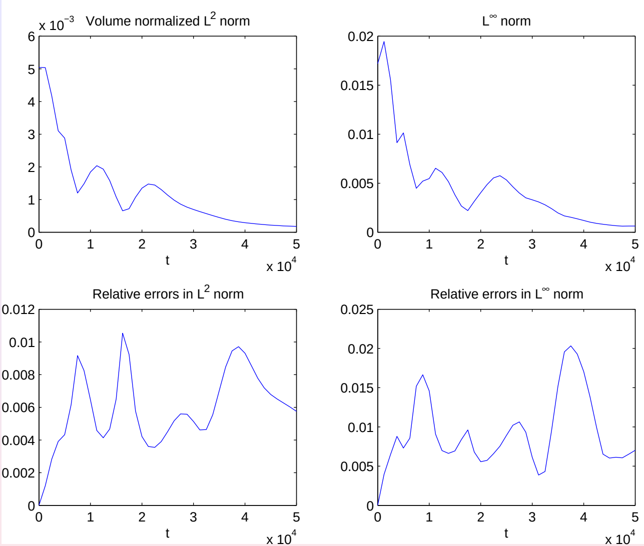

Figure 22: Top row: evolution of the solution ψ in the L^2 and L^∞ norms. Bottom row: evolution of the relative errors for ψ in the L^2 and L^∞ norms.

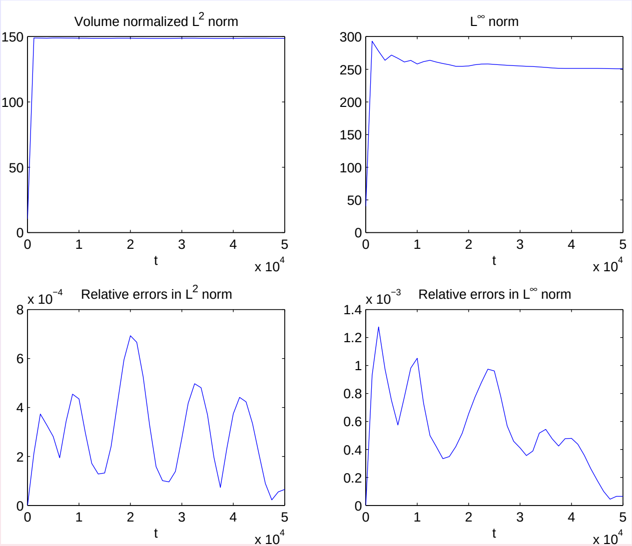

Figure 23: Top row: evolution of the solution ϕ in L^2 and L^∞ norms. Bottom row: evolution of the relative errors for ϕ in L^2 and L^∞ norms.

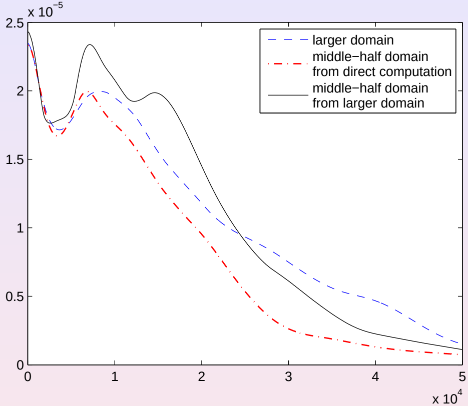

Figure 24: mean divergence

Summary:

- A new set of nonlocal boundary conditions has been implemented.
- We numerically verify that the proposed boundary conditions, proven suitable for the linearized equations, are also suitable for the nonlinear case.
- We numerically verify the transparency property of the proposed boundary conditions.

Thank you !!